

Mini-batch Estimation for Deep Cox Models: Statistical Foundations and Practical Guidance

Lang Zeng

Department of Biostatistics and Health Data Science, University of Pittsburgh

Weijing Tang

Department of Statistics and Data Science, Carnegie Mellon University

Zhao Ren

Department of Statistics, University of Pittsburgh

Ying Ding*

Department of Biostatistics and Health Data Science, University of Pittsburgh

Abstract

The stochastic gradient descent (SGD) algorithm has been widely used to optimize deep Cox neural network (Cox-NN) by updating model parameters using mini-batches of data. We show that SGD aims to optimize the average of mini-batch partial-likelihood, which is different from the standard partial-likelihood. This distinction requires developing new statistical properties for the global optimizer, namely, the mini-batch maximum partial-likelihood estimator (mb-MPLE). We establish that mb-MPLE for Cox-NN is consistent and achieves the optimal minimax convergence rate up to a polylogarithmic factor. For Cox regression with linear covariate effects, we further show that mb-MPLE is \sqrt{n} -consistent and asymptotically normal with asymptotic variance approaching the information lower bound as batch size increases, which is confirmed by simulation studies. Additionally, we offer practical guidance on using SGD, supported by theoretical analysis and numerical evidence. For Cox-NN, we demonstrate that the ratio of the learning rate to the batch size is critical in SGD dynamics, offering insight into hyperparameter tuning. For Cox regression, we characterize the iterative convergence of SGD, ensuring that the global optimizer, mb-MPLE, can be approximated with sufficiently many iterations. Finally, we demonstrate the effectiveness of mb-MPLE in a large-scale real-world application where the standard MPLE is intractable.

Keywords: Cox model; linear scaling rule; minimax rate of convergence; neural network; stochastic gradient descent; survival analysis.

*Corresponding Author Email: yingding@pitt.edu

1 Introduction

Cox proportional hazards regression (Cox 1972) is one of the most commonly used approaches in survival analysis, where the outcome of interest is the time to a certain event. It assumes that the covariates have linear effects on the log-hazard function. With the development of deep learning, Cox deep neural networks (Cox-NN, or deep Cox model) have been proposed to capture the potential nonlinear relationship between covariates and survival outcomes to improve survival prediction accuracy (Faraggi & Simon 1995, Katzman et al. 2018, Ching et al. 2018). Despite the success of the Cox model in survival analysis, it faces a significant optimization challenge when applied to large-scale data. In particular, the Cox model is typically trained by maximizing the partial likelihood (Cox 1975). The maximum partial likelihood estimator (MPLE) is obtained through the gradient descent (GD) algorithm, which requires the entire dataset to compute the gradient. This approach is computationally demanding and memory-intensive, especially with large datasets. For example, in our motivating application, where images are used to predict survival outcomes (as detailed in Section 6), performing GD in Cox-NN with high-dimensional predictors and a large sample size is infeasible due to hardware memory constraints. Even traditional Cox regression faces optimization challenges for large-scale data. Tarkhan & Simon (2024) reported that the GD algorithm for Cox regression is prone to round-off errors when dealing with large sample sizes. Therefore, the scalability of the Cox model is substantially limited by the inefficiencies of GD optimization when applied to large-scale data.

The stochastic gradient descent algorithm (SGD) is a scalable solution for optimization with large-scale data and has been widely used for training NN (Amari 1993, Bottou 2012). SGD alleviates the computational and memory burdens by using a randomly selected (small) subset of the dataset, known as a mini-batch, to compute the gradient and update

parameters in each iteration. Moreover, in NN optimization, [Xie et al. \(2020\)](#) showed that, compared to GD, SGD favors flat minima, which often leads to better generalization. This explains why SGD is preferred for training an NN. However, SGD cannot directly optimize the partial likelihood of all samples through mini-batches because evaluating the partial likelihood of an event subject requires access to data for all subjects who survived longer.

Several attempts have been made to enable parameter updates for Cox models using mini-batch data. [Kvamme et al. \(2019\)](#) followed the idea of nested case-control Cox regression from [Goldstein & Langholz \(1992\)](#), proposing an approximation of the gradient of partial likelihood using the case-control pairs instead of using all at-risk samples. [Sun et al. \(2020\)](#) fitted a Cox-NN to establish a prediction model for an eye disease progression through SGD, where the iteration was based on the partial likelihood of a random subset of data. [Tarkhan & Simon \(2024\)](#) studied SGD for Cox regression in an online learning setting and demonstrated that the gradient of the expected mini-batch partial likelihood at the true parameter is zero. Despite the successful application of SGD to Cox models, the statistical foundations of the mini-batch maximum partial likelihood estimator (mb-MPLE), of which the SGD seeks to estimate, remain unexplored. Notably, the average mini-batch partial likelihood depends on the batch size and differs from the full partial likelihood, as highlighted in [\(2.8\)](#). Such a distinction in the objective function differentiates mb-MPLE from MPLE, requiring the development of new statistical properties for the mb-MPLE.

Motivated by the existing knowledge gap, this work investigated the statistical properties of mb-MPLE for Cox models and provided practical guidance for the SGD application to find the mb-MPLE. Specifically, our contributions come from the following three folds:

- Firstly, for Cox-NN, where the SGD algorithm is commonly used, we establish the consistency and convergence rate of mb-MPLE. Unlike MPLE, which targets the partial likelihood of all samples ([Cox 1975](#)), mb-MPLE minimizes a different objective

function (see (3.2) for details). Consequently, the statistical properties developed for MPLE by Zhong et al. (2022) cannot be applied directly. We demonstrate that the mb-MPLE remains consistent and achieves the minimax optimal convergence rate up to a polylogarithmic factor. The consistency is also supported by numerical evidence. These results provide a statistical foundation for mini-batch estimation in Cox-NN.

- Secondly, we provide practical guidance for training Cox-NN via SGD to search for the mb-MPLE. In practice, both the learning rate and batch size used in SGD are important hyperparameters, as they significantly influence the SGD dynamics. In optimizations where the objective function is independent of batch size, such as empirical risk minimization, *the ratio of the learning rate to the batch size* has been identified as a key factor in SGD dynamics during NN training (Goyal et al. 2017, Jastrzebski et al. 2017, Xie et al. 2020). This observation guides a hyperparameter tuning strategy, where the learning rate or the batch size is fixed while tuning the other. However, for Cox-NN, we note that the function targeted by SGD is batch-size dependent, so it remains unclear whether these results can be applied. To this end, we investigate how the local convexity of the objective changes with the batch size and extend the applicability of the tuning strategy to Cox-NN optimization. We provide both theoretical insights and numerical evidence that *the ratio of the learning rate to the batch size* remains a crucial factor in SGD dynamics during Cox-NN training. This offers insight into Cox-NN hyperparameter tuning.
- Lastly, we develop the statistical properties of mb-MPLE for Cox regression with linear covariate effects. We show that mb-MPLE is \sqrt{n} -consistent and asymptotically normal, with asymptotic variance depending on the batch size. Furthermore, based on theoretical analysis and numerical experiments on the impact of batch size on local

convexity, we demonstrate that doubling the batch size improves the statistical efficiency of mb-MPLE. This phenomenon is not observed in other SGD optimizations, such as empirical risk minimization, where the optimizer’s statistical efficiency is independent of the SGD batch size. Moreover, for Cox regression, we study the numerical convergence of the SGD algorithm to the mb-MPLE. We note that the objective function optimized by SGD is not global strong convex, and an additional projection step is necessary (namely, the *projected SGD*). We follow the non-asymptotic analysis of the projected SGD from [Moulines & Bach \(2011\)](#) to demonstrate that the algorithm approximates the mb-MPLE given sufficiently many iterations.

The rest of the paper is organized as follows. In [Section 2](#), we review the Cox model and the SGD algorithm, with an introduction to the average mini-batch log-partial likelihood and the mb-MPLE for the Cox model. In [Section 3](#), we establish the statistical properties of mb-MPLE for Cox-NN and investigate the impact of SGD batch size on training Cox-NN to find the mb-MPLE. The statistical properties of the mb-MPLE for Cox regression, as well as the convergence of SGD algorithm to the mb-MPLE over iterations, are studied in [Section 4](#). [Section 5](#) presents simulation studies, and [Section 6](#) presents a real-world data analysis. Finally, we conclude and discuss further investigation directions in [Section 7](#).

2 Background and Problem Setup

Let $D(n) = \{D_i\}_{i=1}^n$ denote n independently and identically distributed (i.i.d.) observations. Survival analysis is to analyze the association between the covariate $X \in \mathbb{R}^p$ and the time-to-event outcome T^* (e.g., time-to-death). Let C^* denote the censoring time. Due to the right censoring, the observed time-to-event data is the triplet set $D_i = (X_i, T_i, \Delta_i)$, where $T_i = \min(T_i^*, C_i^*)$ is the observed time and $\Delta_i = I(T_i^* \leq C_i^*)$ is the event indicator.

2.1 Cox Model and Deep Neural Network

The Cox model assumes a multiplicative effect of covariates on the hazard function, i.e.,

$$\lambda(t|X = x) = \lambda_0(t) \exp\{f_0(x)\}, \quad (2.1)$$

where $\lambda_0(t)$ is the baseline hazard function and $f_0(x)$ is the relative risk given covariates x . When assuming the effect of X is linear, i.e., $f_0(X) = X^T\theta_0$, the model (2.1) reduces to the Cox regression model. When the function $f_0(\cdot)$ is unspecified and is modeled through a neural network (NN) f_θ with parameter θ , it is referred to as Cox-NN.

We briefly review the structure of a NN below. Let K be a positive integer and $\mathbf{p} = \{p_0, \dots, p_K, p_{K+1}\}$ be a positive integer sequence. A $(K + 1)$ -layer NN with layer-width \mathbf{p} , i.e., the number of neurons, is a composite function $f : \mathbb{R}^{p_0} \rightarrow \mathbb{R}^{p_{K+1}}$ recursively defined as

$$\begin{aligned} f(x) &= W_K f_K(x) + v_K, \\ f_k(x) &= \sigma(W_{k-1} f_{k-1}(x) + v_{k-1}) \text{ for } k = 2, \dots, K, \\ f_1(x) &= \sigma(W_0 x + v_0), \end{aligned} \quad (2.2)$$

where the matrices $W_k \in \mathbb{R}^{p_{k+1}} \times \mathbb{R}^{p_k}$ and vectors $v_k \in \mathbb{R}^{p_{k+1}}$ (for $k = 0, \dots, K$) are the parameters of the NN. The pre-specified activation function $\sigma(\cdot)$ is a nonlinear transformation that operates component-wise on a vector, that is, $\sigma((x_1, \dots, x_{p_k})^T) = (\sigma(x_1), \dots, \sigma(x_{p_k}))^T$, for $k = 1, \dots, K$. For NN in (2.2), K denotes the depth of the network. The sequence \mathbf{p} lists the width of each layer with the first element p_0 being the dimension of the input variable, p_1, \dots, p_K are the dimensions of the K hidden layers, and p_{K+1} is the dimension of the output layer. The matrix entries $(W_k)_{i,j}$ are the weight linking the j th neuron in layer k to the i th neuron in layer $k + 1$, and the vector entries $(v_k)_i$ represent a shift term associated with the i th neuron in layer $k + 1$. In Cox-NN, the output dimension $p_{K+1} = 1$ since the output $f_\theta(X)$ is a real value. We consider the commonly used activation function

named Rectified Linear Units (ReLU) in [Nair & Hinton \(2010\)](#), i.e., $\sigma(x) = \max\{x, 0\}$, which has been similarly considered in [Schmidt-Hieber \(2020\)](#) and [Zhong et al. \(2022\)](#).

The standard approach to optimizing the Cox model is through minimizing the negative log-partial likelihood function, which is defined as

$$L_{Cox}^{(n)}(\theta) := -\frac{1}{n} \sum_{i=1}^n \Delta_i \log \frac{\exp\{f_\theta(X_i)\}}{\sum_{j=1}^n I(T_j \geq T_i) \exp\{f_\theta(X_j)\}}. \quad (2.3)$$

We refer to the minimizer of (2.3) as the MPLE. In the partial likelihood, sample i who has experienced the event ($\Delta_i = 1$) is compared to all samples that have not yet experienced the event up to time T_i , known as the *at-risk* set. Minimizing (2.3) is typically solved using gradient-descent-based algorithms, where the gradient $\nabla_\theta L_{Cox}^{(n)}(\theta)$ is calculated using all n samples at each iteration ([Therneau et al. 2015](#), [Katzman et al. 2018](#), [Zhong et al. 2022](#)). The consistency and asymptotic normality of the MPLE have been well-studied by [Andersen & Gill \(1982\)](#) for Cox regression. For Cox-NN, the consistency of the MPLE and its convergence rate have been developed by [Zhong et al. \(2022\)](#). However, when optimizing the Cox model through the SGD algorithm using a subset of samples, the algorithm does not directly minimize (2.3), which will be further explained in the next section.

2.2 Stochastic Gradient Descent for Cox Model

The loss function of the Cox model distinguishes its optimization from the typical loss function (e.g., mean squared error (MSE)) when applying the SGD algorithm. In this section, we first provide a brief overview of the SGD algorithm, followed by a discussion of how SGD for the Cox model differs from its standard applications, such as minimizing the MSE, along with the introduction of the mini-batch loss function for Cox model.

Let $L^{(n)}(D(n); \theta)$ be an empirical loss function over n samples to be minimized. In each iteration of the SGD algorithm, the gradient is computed based on a subset of data

$D(s) \subset D(n)$, referred to as a mini-batch, where s denotes the batch size ($1 \leq s \leq n$). Throughout this paper, we assume the batch size s is fixed and is independent of the sample size n . At the $(t + 1)$ -th iteration step of SGD, the parameter is updated through

$$\hat{\theta}_{t+1} = \hat{\theta}_t - \gamma_t \nabla_{\theta} L^{(s)}(D_t(s); \hat{\theta}_t), \quad (2.4)$$

where γ_t is a pre-scheduled learning rate for the t -th iteration. The gradient $\nabla_{\theta} L^{(s)}(D_t(s); \hat{\theta}_t)$ is calculated from the mini-batch data $D_t(s)$ at t -th iterations. Suppose $D_t(s)$ is randomly selected from $D(n)$ with $\nabla_{\theta} L^{(s)}(D_t(s); \hat{\theta}_t)$ uniformly bounded for all t , when $t \rightarrow \infty$, it has been shown that SGD (2.4) with an appropriate learning rate will find the minimizer of $\mathbb{E}_{D_t(s)}[L^{(s)}(D_t(s); \hat{\theta}_t) | D(n)]$ if it is strongly convex, where the expectation is over the randomness of generating $D_t(s)$ from $D(n)$ (Moulines & Bach 2011, Toulis & Airolidi 2017). Throughout the paper, we assume $D_t(s)$ is randomly sampled from $D(n)$ at each iteration, so its distribution is independent of t . To simplify the notation, for any θ , we omit the input data and drop the subscript t and let $L^{(s)}(\theta) := L^{(s)}(D(s); \theta)$, $L^{(n)}(\theta) := L^{(n)}(D(n); \theta)$, and $\mathbb{E}[L^{(s)}(\theta) | D(n)] := \mathbb{E}_{D(s)}[L^{(s)}(D(s); \theta) | D(n)]$.

Take optimizing the MSE for linear regression as an example, the loss function $L_{MSE}^{(n)}(\theta) = \frac{1}{n} \sum_{i=1}^n L_i(\theta)$ is the average of independent individual loss $L_i(\theta) := (Y_i - X_i^T \theta)^2$ which is the discrepancy between the prediction and the observed for subject i . Suppose $D(s)$ is generated by randomly sampling s subjects without replacement from $D(n)$. When optimizing MSE by SGD with the gradient calculated by $\nabla_{\theta} L_{MSE}^{(s)}(\theta) = \frac{1}{s} \sum_{i: D_i \in D(s)} \nabla_{\theta} L_i(\theta)$, SGD optimizes the loss function

$$\begin{aligned} \mathbb{E}[L_{MSE}^{(s)}(\theta) | D(n)] &= \frac{1}{\binom{n}{s}} \sum_{D(s) \subset D(n)} \left\{ \frac{1}{s} \sum_{i: D_i \in D(s)} L_i(\theta) \right\} \\ &= \frac{\binom{n-1}{s-1}}{s \binom{n}{s}} \sum_{i: D_i \in D(n)} L_i(\theta) = \frac{1}{n} \sum_{i: D_i \in D(n)} L_i(\theta) = L_{MSE}^{(n)}(\theta). \end{aligned} \quad (2.5)$$

This suggests that the loss function targeted by SGD coincides with the MSE, so that

minimizers of $\mathbb{E}[L_{MSE}^{(s)}(\theta)|D(n)]$ and $L_{MSE}^{(n)}(\theta)$ exhibit the same statistical properties.

For the Cox model, the SGD implementation (Sun et al. 2020, Tarkhan & Simon 2024) requires at least two samples to calculate the gradient, which restricts $s \geq 2$. The parameters are updated through

$$\hat{\theta}_{t+1} = \hat{\theta}_t - \gamma_t \nabla_{\theta} L_{Cox}^{(s)}(\hat{\theta}_t), \quad (2.6)$$

where the gradient of mini-batch partial likelihood from $D(s)$ is calculated by

$$\nabla_{\theta} L_{Cox}^{(s)}(\theta) := \nabla_{\theta} \left\{ -\frac{1}{s} \sum_{i:D_i \in D(s)} \Delta_i \log \frac{\exp\{f_{\theta}(X_i)\}}{\sum_{j:D_j \in D(s)} I(T_j \geq T_i) \exp\{f_{\theta}(X_j)\}} \right\}. \quad (2.7)$$

and the at-risk set is constructed on $D(s)$. Since the partial likelihood of each individual depends on other at-risk individuals, the average mini-batch partial likelihood does not equal the partial likelihood of the entire dataset. Suppose $D(s)$ is generated by randomly sampling s subjects without replacement from $D(n)$, the SGD recursion (2.6) is to optimize

$$\mathbb{E} \left[L_{Cox}^{(s)}(\theta) | D(n) \right] = \frac{1}{\binom{n}{s}} \sum_{D(s) \subset D(n)} L_{Cox}^{(s)}(\theta) \neq L_{Cox}^{(n)}(\theta). \quad (2.8)$$

As a result, the loss function targeted by SGD differs from the negative log-partial likelihood $L_{Cox}^{(n)}(\theta)$ in (2.3). Therefore, the theoretical results for the MPLE, which minimizes $L_{Cox}^{(n)}(\theta)$, cannot be directly applied to the mb-MPLE, which minimizes $\mathbb{E} \left[L_{Cox}^{(s)}(\theta) | D(n) \right]$. This motivates us to investigate the statistical properties of the mb-MPLE.

3 mb-MPLE for Cox-NN

We first establish the consistency and the convergence rate of the mb-MPLE for Cox-NN in Section 3.1. In Section 3.2, we examine the impact of batch size on Cox-NN training when using SGD to search for the mb-MPLE in practice.

3.1 Statistical Properties of the mb-MPLE

Zhong et al. (2022) studied the asymptotic properties of the MPLE which minimizes (2.3). They showed that the MPLE achieves the minimax optimal convergence rate up to a polylogarithmic factor. While our work is inspired by the theoretical developments in Zhong et al. (2022), it has significant differences. First, the at-risk term $\frac{1}{n} \sum_{j=1}^n I(T_j \geq t) \exp\{f_\theta(X_j)\}$ converges to a fixed function $\mathbb{E}[I(Y > t) \exp\{f_\theta(X)\}]$. However, in the average mini-batch log-partial likelihood, the at-risk term in $L_{Cox}^{(s)}(\theta)$ always consists of s sub-samples. Thus, both the empirical loss $\mathbb{E}[L_{Cox}^{(s)}(\theta)|D(n)]$ and the population loss $\mathbb{E}[L_{Cox}^{(s)}(\theta)]$ depend on s and are different from Zhong et al. (2022). Second, when $D(s)$ is generated by randomly sampling s subjects without replacement from $D(n)$ in each iteration, $\mathbb{E}[L_{Cox}^{(s)}(\theta)|D(n)]$ is an average of $\binom{n}{s}$ combinations of mini-batches, where different batches may share the same samples. Hence, the correlation between batches needs to be handled when deriving the properties of the minimizer of $\mathbb{E}[L_{Cox}^{(s)}(\theta)|D(n)]$.

We impose the following assumptions for the time-to-event data with right censoring:

(A1) The failure time T_i^* and censoring time C_i^* are independent given the covariates X_i .

(A2) There is a truncation time $\tau < \infty$ such that, for some constant $\delta > 0$, $\mathbb{P}(T^* > \tau|X) \geq \delta$ and $\mathbb{P}(\Delta = 1|X) \geq \delta$ almost surely with respect to the probability measure of X .

The stochastic integrals computed from here on will be truncated at this value τ .

(A3) X takes value in a bounded subset of \mathbb{R}^p with probability function bounded away from zero. Without loss of generality, we assume that the domain of X is $[0, 1]^p$.

(A1)-(A3) are common regularity assumptions in survival analysis (Huang 1999, Zhong et al. 2022). (A1) ensures that the censoring mechanism is noninformative. (A2) is a technical assumption that prevents the partial likelihood and score functions from becom-

ing unbounded at the endpoint of the observed event time support. It also ensures the probability of being uncensored is positive regardless of the covariate value.

Following [Schmidt-Hieber \(2020\)](#) and [Zhong et al. \(2022\)](#), we consider a class of NN with sparsity constraints defined as

$$\mathcal{F}(K, \varsigma, \mathbf{p}, \mathcal{D}) = \{f : f \text{ is a DNN with } (K+1) \text{ layers and width vector } \mathbf{p} \text{ such that}$$

$$\max\{\|W_k\|_\infty, \|v_k\|_\infty\} \leq 1\}, \text{ for all } k = 0, \dots, K, \quad (3.1)$$

$$\sum_{k=1}^K \|W_k\|_0 + \|v_k\|_0 \leq \varsigma, \|f\|_\infty \leq \mathcal{D}\},$$

where $\|W_k\|_\infty$ and $\|v_k\|_\infty$ denote the sup-norm of a matrix or vector, $\|\cdot\|_0$ is the number of nonzero entries of a matrix or vector, $\|f\|_\infty$ is the sup-norm of the function f . The constant $\mathcal{D} > 0$ and the sparsity constraint ς is a positive integer. The sparsity assumption is employed due to the widespread application of techniques such as weight pruning ([Srinivas et al. 2017](#)), dropout ([Srivastava et al. 2014](#)), or L_1 regularization. These methods effectively reduce the total number of nonzero parameters, preventing neural networks from overfitting, which results in a sparsely connected NN. We approximate f_0 in (2.1) using a NN $f_\theta \in \mathcal{F}(K, \varsigma, \mathbf{p}, \mathcal{D})$. More precisely, f_0 is estimated by minimizing $\mathbb{E} \left[L_{Cox}^{(s)}(\theta) | D(n) \right]$ through the SGD procedure in (2.6), where $D(s)$ is generated by randomly sampling s subjects without replacement from $D(n)$. To simplify the notation, we omit θ and denote the estimator by

$$\tilde{f}_n^{(s)} = \arg \min_{f \in \mathcal{F}(K, \varsigma, \mathbf{p}, \mathcal{D})} \frac{1}{\binom{n}{s}} \sum_{D(s) \subset D(n)} L_{Cox}^{(s)}(f), \quad (3.2)$$

where $L_{Cox}^{(s)}(f) := \frac{1}{s} \sum_{j: D_j \in D(s)} \Delta_j \left[-f(X_j) + \log \sum_{k: D_k \in D(s)} I(T_k \geq T_j) \exp\{f(X_k)\} \right]$. We use the superscript (s) to indicate its dependency on the batch size s .

We assume f_0 belongs to a composite smoothness function class, which is broad and also assumed by [Zhong et al. \(2022\)](#). Specifically, let $\mathcal{H}_r^\alpha(\mathbb{D}, M)$ be a Hölder class of smooth

functions with parameters $\alpha, M > 0$ and domain $\mathbb{D} \subseteq \mathbb{R}^r$ defined by

$$\mathcal{H}_r^\alpha(\mathbb{D}, M) = \left\{ h : \mathbb{D} \rightarrow \mathbb{R} : \sum_{\beta: |\beta| < \alpha} \|\partial^\beta h\|_\infty + \sum_{\beta: |\beta| = \lfloor \alpha \rfloor} \sup_{x, y \in \mathbb{D}, x \neq y} \frac{|\partial^\beta h(x) - \partial^\beta h(y)|}{\|x - y\|_\infty^{\alpha - \lfloor \alpha \rfloor}} \leq M \right\},$$

where $\lfloor \alpha \rfloor$ is the largest integer strictly smaller than α , $\partial^\beta := \partial^{\beta_1} \dots \partial^{\beta_r}$ with $\beta = (\beta_1, \dots, \beta_r)$, and $|\beta| = \sum_{k=1}^r \beta_k$.

Let $q \in \mathbb{N}$, $\vec{\alpha} = (\alpha_0, \dots, \alpha_q) \in \mathbb{R}_+^{q+1}$ and $\mathbf{d} = (d_0, \dots, d_{q+1}) \in \mathbb{N}_+^{q+2}$, $\tilde{\mathbf{d}} = (\tilde{d}_0, \dots, \tilde{d}_q) \in \mathbb{N}_+^{q+1}$ with $\tilde{d}_j \leq d_j, j = 0, \dots, q$, where \mathbb{R}_+ is the set of all positive real numbers. The composite smoothness function class is

$$\begin{aligned} \mathcal{H}(q, \vec{\alpha}, \mathbf{d}, \tilde{\mathbf{d}}, M) &:= \{h = h_q \circ \dots \circ h_0 : h_i = (h_{i1}, \dots, h_{id_{i+1}})^T \text{ and} \\ &h_{ij} \in \mathcal{H}_{\tilde{d}_i}^{\alpha_i}([a_i, b_i]^{\tilde{d}_i}, M), \text{ for some } |a_i|, |b_i| \leq M\}, \end{aligned} \quad (3.3)$$

where $\tilde{\mathbf{d}}$ is the intrinsic dimension of the function. For example, if

$$f(x) = f_{21}(f_{11}(f_{01}(x_1, x_2), f_{02}(x_3, x_4)), f_{12}(f_{03}(x_5, x_6), f_{04}(x_7, x_8))) \quad x \in [0, 1]^8,$$

and f_{ij} are twice continuously differentiable, then the smoothness parameter $\alpha = (2, 2, 2)$, the dimension vectors $\mathbf{d} = (8, 4, 2, 1)$ and $\tilde{\mathbf{d}} = (2, 2, 2)$. We assume that

(N1) The unknown function f_0 is an element of $\mathcal{H}_0 = \{f \in \mathcal{H}(q, \vec{\alpha}, \mathbf{d}, \tilde{\mathbf{d}}, M) : \mathbb{E}[f(X)] = 0\}$.

The mean zero constraint in (N1) is for the identifiability of f_0 since the presence of two unknown functions in (2.1).

We denote $\tilde{\alpha}_i = \alpha_i \prod_{k=i+1}^q (\alpha_k \wedge 1)$ and $\Upsilon_n = \max_{i=0, \dots, q} n^{-\tilde{\alpha}_i / (2\tilde{\alpha}_i + \tilde{d}_i)}$ with notation $a \wedge b := \min\{a, b\}$. Furthermore, we denote $a_n \lesssim b_n$ as $a_n \leq cb_n$ for some constant $c > 0$ and any n . $a_n \asymp b_n$ means $a_n \lesssim b_n$ and $b_n \lesssim a_n$. We assume the following NN structure:

(N2) $K = O(\log n)$, $\varsigma = O(n\Upsilon_n^2 \log n)$ and $n\Upsilon_n \lesssim \min(p_k)_{k=1, \dots, K} \leq \max(p_k)_{k=1, \dots, K} \lesssim n$.

A large neural network leads to a smaller approximation error and a larger estimation error.

(N2) defines the structure of the NN family in (3.1) and was also adopted in Zhong et al. (2022) to balance the trade-off between approximation and estimation errors.

We first present a lemma that is critical to studying the asymptotic properties of $\tilde{f}_n^{(s)}$:

Lemma 1. *Let $L_0^{(s)}(f) := \mathbb{E}[L_{Cox}^{(s)}(f)] = \mathbb{E}_{D(n)} \left[\mathbb{E} \left[L_{Cox}^{(s)}(\theta) | D(n) \right] \right]$. Under the Cox model, with assumptions (A1)-(A3) and (N1), for any integer $s \geq 2$ and constant $c > 0$, we have*

$$L_0^{(s)}(f) - L_0^{(s)}(f_0) \asymp d^2(f, f_0)$$

for all $f \in \{f : \|f\|_\infty \leq c, \mathbb{E}[f(X)] = 0\}$, where $d(f, f_0) = [\mathbb{E}\{f(X) - f_0(X)\}^2]^{\frac{1}{2}}$.

Remark 1. *Suppose $\tilde{f}^{(s)} = \arg \min_{f: \|f\|_\infty \leq c, \mathbb{E}[f(X)] = 0} L_0^{(s)}(f)$ and by definition $L_0^{(s)}(\tilde{f}^{(s)}) \leq L_0^{(s)}(f_0)$. On the other hand, we have $L_0^{(s)}(\tilde{f}^{(s)}) \geq L_0^{(s)}(f_0)$ from Lemma 1. Hence, $L_0^{(s)}(\tilde{f}^{(s)}) - L_0^{(s)}(f_0) = 0$ and it implies $\tilde{f}^{(s)} = f_0$. That is, for any integer $s \geq 2$, the minimizer of $L_0^{(s)}(f)$ on a neighborhood of f_0 is f_0 and does not depend on s . Our result can be viewed as a generalization of the result in [Tarkhan & Simon \(2024\)](#), where they consider a parametric function f_θ with the truth $f_0 = f_{\theta_0}$ and demonstrate that $\nabla_\theta L_0^{(s)}(f_\theta)|_{\theta=\theta_0} = 0$.*

Next, we establish the consistency of the mb-MPLE $\tilde{f}_n^{(s)}$ defined in (3.2) for Cox-NN. Note that the expectation of the estimator $\tilde{f}_n^{(s)}$ in (3.2) is not necessarily zero. For the identifiability condition $\mathbb{E}[f_0] = 0$ in (N2), we apply a mean shift by subtracting the empirical average $\tilde{f}_n^{(s)} := \frac{1}{n} \sum_{i=1}^n \tilde{f}_n^{(s)}(X_i)$ ba. The following theorem gives the convergence rate of the mean-shifted mb-MPLE. This is different from [Zhong et al. \(2022\)](#), where the convergence rate was established for the MPLE after shifting by the true mean.

Theorem 1. *Under the Cox model, with assumptions (A1)-(A3) and (N1)-(N2), for any integer $s \geq 2$, we have*

$$\|(\tilde{f}_n^{(s)} - \tilde{f}_n^{(s)}) - f_0\|_{L^2([0,1]^p)} = O_p(\Upsilon_n \log^2 n).$$

Remark 2. *For any integer $s \geq 2$, the convergence rate of $\tilde{f}_n^{(s)}$ is the same as the MPLE in [Zhong et al. \(2022\)](#). The rate is determined by the smoothness and the intrinsic dimension $\tilde{\mathbf{d}}$ of the function f_0 , rather than the dimension \mathbf{d} . Therefore, the estimator $\tilde{f}_n^{(s)}$ can*

circumvent the curse of dimensionality (Bauer & Kohler 2019) and has a fast convergence rate when the intrinsic dimension is low. The batch size s only implicitly influences the constant of the rate. Later, as we consider the parametric Cox model in Section 4, the impact of s on the asymptotic variance of the estimator becomes more apparent.

Remark 3. The minimax lower bound for estimating f_0 can be derived following the proof of Theorem 3.2 in Zhong et al. (2022) as their Lemma 4 and derivations still hold without the parametric linear term. Specifically, let $\Omega_0 = \{\lambda_0(t) : \int_0^\infty \lambda_0(s)ds < \infty \text{ and } \lambda_0(t) \geq 0 \text{ for } t \geq 0\}$. Under the Cox model with assumptions (A1)-(A3) and (N1), there exists a constant $c > 0$, such that $\inf_{\hat{f}} \sup_{(\lambda_0, f_0) \in \Omega_0 \times \mathcal{H}_0} \mathbb{E}\{\hat{f}(X) - f_0(X)\}^2 \geq c\gamma_n^2$, where the infimum is taken over all possible estimators \hat{f} based on the observed data. Thus, the NN-estimator is rate-optimal as it attains the minimax lower bound up to a polylogarithm factor.

Remark 4. We note that Theorem 1 established the properties for the global optimal $\tilde{f}_n^{(s)}$. In practice, however, NN training involves solving a challenging non-convex optimization problem, and the SGD does not generally guarantee convergence to the global minimum. As a result, there may be an optimization error between the SGD output $\hat{f}_n^{(s)}$ and the mb-MPLE $\tilde{f}_n^{(s)}$. In the case of Cox regression, where the optimization problem is convex, we showed in Theorem 4 that SGD converges to the global optimum given sufficient iterations. For the general non-convex setting in Cox-NN, the optimization error depends on factors, such as the learning rate and initialization (see Choromanska et al. (2015), Kleinberg et al. (2018), Schmidt-Hieber (2020) for more discussion). We leave the analysis of the optimization error in Cox-NN for future work.

We conducted simulations to numerically verify the Theorem 1 by evaluating the root mean squared error (RMSE) and prediction performance of the estimator $\hat{f}^{(s)} - \tilde{f}^{(s)}$, given by SGD, under different training sample sizes n with different choices of s . Across various

choices of s , as the training sample size increases, the RMSE decreases, and the prediction accuracy is improved on holdout test data (see details in the Supplementary Material).

3.2 Impact of Batch Size on Cox-NN Training

The previous section focuses on the statistical properties of the mb-MPLE $\tilde{f}_n^{(s)}$, the global minimizer of (3.2). In practice, searching for the mb-MPLE through SGD is challenging since the NN training is a highly non-convex optimization problem and can be affected by many factors (Li et al. 2018). It has been noticed that the ratio of the learning rate to the batch size γ/s is a key factor that determines SGD dynamics (Goyal et al. 2017, Jastrzebski et al. 2017). Goyal et al. (2017) demonstrates that keeping γ/s constant makes the SGD training process almost unchanged on a broad range of batch sizes, which is known as the *linear scaling rule*. This rule guides hyperparameter tuning in NN such that we can fix either γ or s and only tune the other parameter to optimize the behavior of SGD.

It remains unclear whether the linear scaling rule can be applied to Cox-NN training, as the population loss $\mathbb{E}[L_{Cox}^{(s)}(\theta)]$ in Cox-NN depends on the batch size. When applying SGD in training a neural network f_θ with a specified structure, we treat the parameter θ as finite-dimensional. Existing theoretical work focused on the population loss $\mathbb{E}[L(\theta)]$ which is invariant to different batch sizes and assumed that the Hessian equals the covariance of gradient at the truth, that is $\nabla_\theta^2 \mathbb{E}[L(\theta)]|_{\theta=\theta_0} = \mathbb{V}[\nabla_\theta L(\theta)]|_{\theta=\theta_0}$ (Jastrzebski et al. 2017, Xie et al. 2020). These key properties of the objective function are violated for the population loss $\mathbb{E}[L_{Cox}^{(s)}]$ under the Cox model, as shown in the following theorem.

Theorem 2. *Under the Cox model with $f_0 = f_{\theta_0}$ parameterized by θ_0 of finite dimension, with assumptions (A1)-(A3) and suppose $\nabla_\theta f_\theta$, $\nabla_\theta^2 f_\theta$ exist and $f_\theta, \nabla_\theta f_\theta$, $\nabla_\theta^2 f_\theta$ are element-wise bounded for all X on a neighborhood of θ_0 with $\nabla_\theta^2 \mathbb{E}[L_{Cox}^{(s)}(\theta)]|_{\theta=\theta_0}$ being posi-*

tive definite, then for any integer $s \geq 2$ we have

$$\nabla_{\theta}^2 \mathbb{E}[L_{Cox}^{(s)}(\theta)]|_{\theta=\theta_0} = s \mathbb{V}[\nabla_{\theta} L_{Cox}^{(s)}(\theta)]|_{\theta=\theta_0}, \quad (3.4)$$

$$\nabla_{\theta}^2 \mathbb{E}[L_{Cox}^{(2s)}(\theta)]|_{\theta=\theta_0} \succeq \nabla_{\theta}^2 \mathbb{E}[L_{Cox}^{(s)}(\theta)]|_{\theta=\theta_0}, \quad (3.5)$$

where \mathbb{V} denotes the variance, ∇_{θ}^2 is second-order derivative operator with respect to θ and $A \succeq B$ denotes $A - B$ is positive semi-definite.

Remark 5. For i th individual loss L_i , the property $\nabla_{\theta}^2 \mathbb{E}[L_i(\theta)]|_{\theta=\theta_0} = \mathbb{V}[\nabla_{\theta} L_i(\theta)]|_{\theta=\theta_0}$ immediately implies $\nabla_{\theta}^2 \mathbb{E}[\frac{1}{s} \sum_{i=1}^s L_i(\theta)]|_{\theta=\theta_0} = s \mathbb{V}[\nabla_{\theta} \frac{1}{s} \sum_{i=1}^s L_i(\theta)]|_{\theta=\theta_0}$ for any mini-batch of s i.i.d. samples. The equality (3.4) indicates this batch-level relation still holds for the negative-log-partial likelihood, which is useful to study the SGD dynamic (Jastrzebski et al. 2017, Xie et al. 2020). Moreover, the inequality (3.5) and Remark 1 together depict the properties of $\mathbb{E}[L_{Cox}^{(s)}(\theta)]$. The global minimizer of $\mathbb{E}[L_{Cox}^{(s)}(\theta)]$ is always θ_0 , which does not depend on the batch size s , while the local convexity of $\mathbb{E}[L_{Cox}^{(s)}(\theta)]$ increases when s doubles. Figure 1a presents an illustrative picture of $\mathbb{E}[L_{Cox}^{(s)}(\theta)]$ showing these two properties.

The relation (3.5) is only established at the true θ_0 , but it gives us the intuition that the convexity of $\mathbb{E}[L_{Cox}^{(s)}(\theta)]$ increases when s increases. Nevertheless, we show that the convexity change is negligible when s is large, as shown in the following proposition:

Proposition 1. Let $H_s = \nabla_{\theta}^2 \mathbb{E}[L_{Cox}^{(s)}(\theta)]|_{\theta=\theta_0}$ and let $Tr(\cdot)$ denote the trace. Under the Cox model with the assumptions in Theorem 2 hold, then $Tr(H_{2s}) - Tr(H_s) \lesssim 1/s$.

The Proposition 1 suggests that, when s is sufficiently large, we can treat $\nabla_{\theta}^2 \mathbb{E}[L_{Cox}^{(s)}(\theta)]$ as approximately invariant to s , allowing existing insights on SGD to extend to Cox-NN. Following Jastrzebski et al. (2017), we approximate the SGD by a stochastic differential equation and show that the linear scaling rule for Cox-NN training remains approximately valid when the batch size is large (see details in the Supplementary Material). This is

numerically verified in Section 5. As a hyperparameter tuning strategy, we can fix either γ or s and only tune the other to optimize the behavior of SGD. This strategy reduces one hyperparameter to be tuned in Cox-NN training.

4 mb-MPLE for Cox Regression

In this section, we further establish the asymptotic normality of the mb-MPLE for Cox regression, where the linear effect of covariates is assumed. Specifically, we study the impact of s on the asymptotic variance of the linear coefficient estimator and the convergence of the SGD algorithm over iterations. We consider the Cox regression model with $f(X) = \theta_0^T X$ and estimate θ_0 through the SGD procedure (2.6) with

$$\nabla_{\theta} L_{Cox}^{(s)}(\theta) := -\frac{1}{s} \sum_{i: D_i \in D(s)} \Delta_i \left[X_i - \frac{\sum_{j: D_j \in D(s)} I(T_j \geq T_i) \exp\{\theta^T X_j\} X_j}{\sum_{j: D_j \in D(s)} I(T_j \geq T_i) \exp\{\theta^T X_j\}} \right]. \quad (4.1)$$

We assume the following assumptions for the regression setting:

- (R1) The true parameter θ_0 associated with the relative risk $f_0(X) = \theta_0^T X$ is an interior point of $\mathbb{R}_M^p := \{\theta \in \mathbb{R}^p : \|\theta\|_2 \leq M\}$.
- (R2) There exist constants $0 < c_1 < c_2 < \infty$ such that the subdensities $p(x, t, \Delta = 1)$ of $(X, T, \Delta = 1)$ satisfies $c_1 < p(x, t, \Delta = 1) < c_2$ for all $(x, t) \in [0, 1]^p \times [0, \tau]$.

The subdensity $p(x, t, \Delta = \delta)$ is defined as

$$p(x, t, \Delta = \delta) = \frac{\partial^2 \mathbb{P}(X \leq x, T \leq t, \Delta = \delta)}{\partial t \partial x}.$$

Assumptions (R1) and (R2) are sufficient to demonstrate the strong convexity of $\mathbb{E}[L_{Cox}^{(s)}(\theta)]$ on any compact subspace of \mathbb{R}^p , so that $\mathbb{E}[\nabla_{\theta}^2 L_{Cox}^{(s)}(\theta)]|_{\theta=\theta_0} \succ 0$ and θ_0 is identifiable. See Lemma 2 for the details.

Next, depending on the nature of data collection, we study the mb-MPLE for Cox regression under the offline scenario (unstreaming data) and the online scenario (streaming data). In the first scenario, the entire dataset $D(n)$ of n i.i.d. samples has been collected. In the second scenario, the observations arrive in a continual stream of strata, and the model is continuously updated as new data arrives without storing the entire dataset.

4.1 Offline Cox Regression

To study the statistical properties of $\tilde{\theta}_n^{(s)} := \arg \min_{\theta} \mathbb{E}[L_{Cox}^{(s)}(\theta)|D(n)]$, we consider two sampling strategies of $D(s)$ from $D(n)$ which determines the form of $\mathbb{E}[L_{Cox}^{(s)}(\theta)|D(n)]$. The first strategy has been considered in Theorem 1 where $D(s)$ is generated by randomly sampling s subjects from $D(n)$ without replacement. We refer to it as a stochastic batch (SB) with the estimator

$$\tilde{\theta}_n^{SB(s)} = \arg \min_{\theta \in \mathbb{R}_M^p} \frac{1}{\binom{n}{s}} \sum_{D(s) \subset D(n)} L_{Cox}^{(s)}(\theta). \quad (4.2)$$

Another popular strategy in SGD applications is to randomly split the whole sample into $m = n/s$ non-overlapping batches. Once the mini-batches are established, they are fixed and then repeatedly used throughout the rest of the algorithm (Qi et al. 2023). We refer to it as a fixed batch (FB) with the estimator

$$\tilde{\theta}_n^{FB(s)} = \arg \min_{\theta \in \mathbb{R}_M^p} \frac{1}{m} \sum_{D(s) \in D(n|s)} L_{Cox}^{(s)}(\theta), \quad (4.3)$$

where we use $D(n|s)$ to denote that $D(n)$ has been partitioned into $m = n/s$ fixed disjoint batches. The element of $D(n|s)$ is a mini-batch containing s i.i.d. samples and $D(s)$ is generated by randomly picking one element from $D(n|s)$. The impact of batch size on the asymptotic variance of $\tilde{\theta}_n^{FB(s)}$ can be well-established.

We present the asymptotic properties of $\tilde{\theta}_n^{SB(s)}$ and $\tilde{\theta}_n^{FB(s)}$ in the following theorem:

Theorem 3. Under the Cox model, with assumptions (A1)-(A3) and (R1)-(R2), for any integer $s \geq 2$, we have

$$\sqrt{n}(\tilde{\theta}_n^{SB(s)} - \theta_0) \rightarrow^d N(0, s^2 H_s^{-1} \Sigma_{(s|1)} (H_s^{-1})^T), \quad (4.4)$$

$$\sqrt{n}(\tilde{\theta}_n^{FB(s)} - \theta_0) \rightarrow^d N(0, s H_s^{-1} \Sigma_s (H_s^{-1})^T), \quad (4.5)$$

when $n \rightarrow \infty$, where $H_s = \mathbb{E}[\nabla_\theta^2 L_{Cox}^{(s)}(\theta)]|_{\theta=\theta_0}$, $\Sigma_s = \mathbb{V}[\nabla_\theta L_{Cox}^{(s)}(\theta)]|_{\theta=\theta_0}$, and

$$\Sigma_{(s|1)} = \mathbb{V} \left\{ \nabla_\theta L_{Cox}^{(s)}(D_{i_1}, D_{i_2}, \dots, D_{i_s} | \theta), \nabla_\theta L_{Cox}^{(s)}(D_{i_1}, \tilde{D}_{i_2}, \dots, \tilde{D}_{i_s} | \theta) \right\} \Big|_{\theta=\theta_0},$$

which is the covariance of $\nabla_\theta L_{Cox}^{(s)}$ on two mini-batches $D(s)$ sharing the same sample D_{i_1} but different rest $s - 1$ samples (denoted by \tilde{D}).

Remark 6. Theorem 3 states that, for any choice of batch size s , both $\tilde{\theta}_n^{SB(s)}$ and $\tilde{\theta}_n^{FB(s)}$ are \sqrt{n} -consistent, asymptotically normal with a sandwich-type variance while the middle part of the asymptotic variance differs. By the theory of the U-statistics (Hoeffding 1992), we have $s^2 \Sigma_{(s|1)} \preceq s \Sigma_s$ and the equality holds only if $\nabla_\theta L^{(s)}(\theta)$ can be written as the average of s i.i.d. gradients, such as MSE in (2.5). Because this condition does not hold for $\nabla_\theta L_{Cox}^{(s)}(\theta)$ presented in (2.7), it implies that $s^2 H_s^{-1} \Sigma_{(s|1)} (H_s^{-1})^T \prec s H_s^{-1} \Sigma_s (H_s^{-1})^T$ and, thus, $\tilde{\theta}_n^{SB(s)}$ is asymptotically more efficient than $\tilde{\theta}_n^{FB(s)}$. The FB strategy ignores the ranking between samples from different non-overlapping batches. This loss of information consequently reduces the efficiency. Note that this phenomenon is not typically observed in SGD optimizations. Take the MSE in (2.5) for instance, one can verify that $s^2 H_s^{-1} \Sigma_{(s|1)} (H_s^{-1})^T = s H_s^{-1} \Sigma_s (H_s^{-1})^T$ and $\tilde{\theta}_n^{FB(s)}$ is therefore as efficient as $\tilde{\theta}_n^{SB(s)}$.

Remark 7. The convergence rate established in Theorem 1 still holds if we consider the FB strategy for NN training and replace the empirical loss in (3.2) by $\frac{1}{m} \sum_{D(s) \in D(n|s)} L_{Cox}^{(s)}(f)$. The proof is simpler because there are no correlations between the batches, and the empirical loss is the average of m i.i.d. tuples. Hence, the convergence rate is $O_p(\gamma_m \log^2 m)$, which is equivalent to $O_p(\Upsilon_n \log^2 n)$ as $m = n/s$ with s being a fixed constant.

Remark 8. We extend our results for the mb-MPLE to the partially linear Cox model considered by [Zhong et al. \(2022\)](#), where $\lambda(t|X, Z) = \lambda_0(t) \exp\{\theta_0^T Z + f_0(X)\}$ including both the linear component $\theta_0^T Z$ and the nonlinear component $f_0(X)$, and we find similar statistical properties of mb-MPLE as shown in this work. Specifically, the NN estimator of the nonlinear component achieves the minimax optimal rate of convergence while the finite-dimensional estimator for the linear covariate effect is \sqrt{n} -consistent and asymptotically normal with variance depending on the batch size (see details in Supplementary Material). This result integrates [Theorem 1](#) for the nonparametric Cox model and [Theorem 3](#) for the parametric Cox model.

Remark 9. By [Theorem 2](#), we have

$$H_s = \mathbb{E}[\nabla_{\theta}^2 L_{Cox}^{(s)}(\theta)]|_{\theta=\theta_0} = s\mathbb{V}[\nabla_{\theta} L_{Cox}^{(s)}(\theta)]|_{\theta=\theta_0} = s\Sigma_s, \quad (4.6)$$

$$H_{2s} = \mathbb{E}[\nabla_{\theta}^2 L_{Cox}^{(2s)}(\theta)]|_{\theta=\theta_0} \succeq \mathbb{E}[\nabla_{\theta}^2 L_{Cox}^{(s)}(\theta)]|_{\theta=\theta_0} = H_s. \quad (4.7)$$

Equality (4.6) indicates that the asymptotic variance of $\tilde{\theta}_n^{FB(s)}$ is $sH_s^{-1}\Sigma_s(H_s^{-1})^T = H_s^{-1}$. Then by (4.7), we have $H_{2s}^{-1} \preceq H_s^{-1}$, i.e., the asymptotic efficiency of $\tilde{\theta}_n^{FB(s)}$ improves when the s doubles. The asymptotic variance of $\tilde{\theta}_n^{SB(s)}$ cannot be further simplified to directly evaluate the impact of batch size. Nevertheless, the decrease of its upper bound $sH_s^{-1}\Sigma_s(H_s^{-1})^T$ implies the efficiency improvement when batch size doubles. Moreover, such an impact of batch size on the asymptotic variance is, again, not typically observed in SGD optimizations. Taking the MSE in (2.5) as an example, one can verify that $sH_s^{-1}\Sigma_s(H_s^{-1})^T$ degenerates to $H_1^{-1}\Sigma_1(H_1^{-1})^T$, which does not depend on s . The efficiency improvement of the mb-MPLE is because the objective function $\mathbb{E}[\nabla_{\theta} L_{Cox}^{(s)}(\theta)]$ gets closer to the efficient score function ([Tsiatis 2006](#)) for Cox regression when s increases.

Remark 10. One can verify that

$$\mathbb{E}[\nabla_{\theta}^2 L_{Cox}^{(s)}(\theta)]|_{\theta=\theta_0} \rightarrow I(\theta_0) \text{ and } s\mathbb{V}[\nabla_{\theta} L_{Cox}^{(s)}(\theta)]|_{\theta=\theta_0} \rightarrow I(\theta_0) \text{ when } s \rightarrow \infty,$$

where $I(\theta_0)$ is the information matrix of θ_0 . This implies that H_s^{-1} decreases towards its lower bound $I(\theta_0)^{-1}$ as s continues to double, suggesting that the mb-MPLE is less efficient than the MPLE, whose asymptotic variance is $I(\theta_0)^{-1}$. On the other hand, when the batch size is large and H_s^{-1} is approaching $I(\theta_0)^{-1}$, the efficiency gain from doubling the batch size would diminish, which has been empirically reported in [Tarkhan & Simon \(2024\)](#).

4.2 Online Cox Regression

In contrast to the offline Cox regression, which minimizes the empirical loss $\mathbb{E}[L_{Cox}^{(s)}(\theta)|D(n)]$ with given $D(n)$, the online Cox regression minimizes the population loss $\mathbb{E}[L_{Cox}^{(s)}(\theta)]$ by directly sampling the mini-batch $D(s)$ from the population. For online learning, it is of interest to study the convergence of $\hat{\theta}_t$ to θ_0 when the iteration step $t \rightarrow \infty$, where $\hat{\theta}_t$ is the estimator at the t -th iteration in SGD. This is an optimization problem of whether an algorithm can reach the global minimizer over the iterations. It differs from our previous investigation of an estimator's asymptotic properties when the sample size goes to infinity.

The strong convexity of the objective function has been widely used to establish the fast convergence of SGD algorithm to the global minimizer ([Ruppert 1988](#), [Polyak & Juditsky 1992](#), [Moulines & Bach 2011](#), [Toulis & Airoidi 2017](#)). It requires the function to grow as fast as a quadratic function. Specifically, a function $h(x)$ is strongly convex over a domain \mathcal{X} if there exists a constant $\mu > 0$ such that its Hessian satisfies $\nu^T \nabla_x^2 h(x) \nu \geq \mu > 0$ for any $x \in \mathcal{X}$ and vector $\nu \in \{\nu : \|\nu\|_2 = 1\}$, where $\|\cdot\|_2$ denotes the Euclidean norm. In our case, the population loss of online Cox regression $\mathbb{E}[L_{Cox}^{(s)}(\theta)] = \mathbb{E} \left[-\frac{1}{s} \sum_{i: D_i \in D(s)} \Delta_i \log \frac{\exp(\theta^T X_i)}{\sum_{j: D_j \in D(s)} I(T_j \geq T_i) \exp(\theta^T X_j)} \right]$ is not strongly convex globally over \mathbb{R}^p . For example, when $p = 1$, it is straightforward to verify that $\mathbb{E}[L_{Cox}^{(s)}(\theta)] = O(\theta)$ and the Hessian vanishes when $\theta \rightarrow \infty$, hence the global strong convexity does not hold. However, we show that $\mathbb{E}[L_{Cox}^{(s)}(\theta)]$ is strongly convex within any ball centered at the origin

that contains the true parameter θ_0 . This local strong convexity facilitates the application of existing SGD convergence results to the Cox regression setting.

Lemma 2. *Suppose the integer $s \geq 2$, the constant $B > 0$, and $\theta_0 \in \mathbb{R}_B^p := \{\theta \in \mathbb{R}^p : \|\theta\|_2 \leq B\}$. Under Cox regression, with assumptions (A1)-(A3), (R1), (R2), there exist a constant $\mu > 0$ such that for any $\theta \in \mathbb{R}_B^p$*

$$\nu^T \mathbb{E}[\nabla_{\theta}^2 L_{Cox}^{(s)}(\theta)] \nu \geq \mu > 0, \quad \forall \nu \in \{\nu : \|\nu\|_2 = 1\}.$$

The radius $B > 0$ can be arbitrarily large so that \mathbb{R}_B^p covers the true parameter θ_0 to guarantee $\mathbb{E}[L_{Cox}^{(s)}(\theta)]$ is strongly convex on \mathbb{R}_B^p . Therefore, a modification of (2.6) could be applied to restrict the domain of θ and, hence, to establish the fast convergence of the SGD algorithm for Cox regression, which is called projected SGD. That is,

$$\hat{\theta}_{t+1} = \Pi_{\mathbb{R}_B^p}[\hat{\theta}_t - \gamma_t \nabla_{\theta} L_{Cox}^{(s)}(\hat{\theta}_t)], \quad (4.8)$$

where $\Pi_{\mathbb{R}_B^p}$ is the orthogonal projection operator on the ball $\mathbb{R}_B^p := \{\theta \in \mathbb{R}^p : \|\theta\|_2 \leq B\}$ (Moulines & Bach 2011). The projection step keeps iterates within the area where the local strong convexity of $\mathbb{E}[L_{Cox}^{(s)}(\theta)]$ holds. By applying Theorem 2 of Moulines & Bach (2011), we obtain the following non-asymptotic result with respect to the iteration step t .

Theorem 4. *Consider the SGD procedure (4.8) with learning rate $\gamma_t = \frac{C}{t^\alpha}$ where the constant $C > 0$ and $\alpha \in [0, 1]$. Under the Cox regression, with assumptions (A1)-(A3), (R1)-(R2), and assume $\|\theta_0\| \leq B$, then for any integer $s \geq 2$, we have*

$$\mathbb{E}\|\hat{\theta}_t - \theta_0\|^2 \leq \begin{cases} \{\delta_0^2 + D^2 C^2 \varphi_{1-2\alpha}(t)\} \exp(-\frac{\mu C}{2} t^{1-\alpha}) + \frac{2D^2 C^2}{\mu t^\alpha} & \text{if } \alpha \in [0, 1); \\ \delta_0^2 t^{-\mu C} + 2D^2 C^2 t^{-\mu C} \varphi_{\mu C-1}(t) & \text{if } \alpha = 1, \end{cases} \quad (4.9)$$

where δ_0 is the distance between the initialization of SGD and θ_0 , $D = \max_{\theta \in \mathbb{R}_B^p, D(s)} \|\nabla_{\theta} L_{Cox}^{(s)}(\theta)\|$, and μ is the strong-convexity constant in Lemma 2. The function $\varphi_{\beta}(t) : \mathbb{R}^+ \setminus \{0\} \rightarrow \mathbb{R}$ is

given by

$$\varphi_\beta(t) = \begin{cases} \frac{t^\beta - 1}{\beta} & \text{if } \beta \neq 0, \\ \log t & \text{if } \beta = 0. \end{cases}$$

Remark 11. *This result ensures that for Cox regression, the global minimizer of $\mathbb{E}[L_{Cox}^{(s)}(\theta)]$ can be approximated by the projected SGD algorithm with a large enough number of iterations. Specifically, the upper bound in (4.9) goes to 0 when α is not 0. When $\alpha \in (0, 1)$, the convergence is at rate $O(\frac{1}{t^\alpha})$. When $\alpha = 1$, the convergence rate is $O(\frac{1}{t})$ if $\mu C > 1$, the convergence rate is $O(\frac{\log t}{t})$ if $\mu C = 1$, and is $O(\frac{1}{t\mu C})$ if $\mu C < 1$. The learning rate can be set as $\gamma_t = \frac{C}{t}$ with a large constant C to achieve the optimal convergence rate.*

Remark 12. *The high-probability error bound for the projected SGD estimator is also derived and presented in the online Supplementary Materials. Additionally, we show that the running average SGD (ASGD) estimator $\bar{\theta}_t = \frac{1}{t} \sum_{k=1}^t \hat{\theta}_k$ (no projection), achieves the optimal $O(t^{-1})$ rate and $\sqrt{t}(\bar{\theta}_t - \theta_0)$ is asymptotically normal for $\gamma_t = \frac{C}{t^\alpha}$ with $\alpha \in (0.5, 1)$ and $C > 0$. This is useful for uncertainty quantification in online Cox regression (see Supplementary Materials).*

Remark 13. *The convergence of SGD for offline Cox regression can be similarly established. If $D(s)$ is sampled from the $D(n)$ using either method considered in Section 4.1, and if $\tilde{\theta}_n := \arg \min_{\theta} \mathbb{E}[L_{Cox}^{(s)}(\theta) | D(n)]$ is finite, then the expected distance between $\hat{\theta}_t$ and $\tilde{\theta}_n$ converges over the iterations (4.8). This justifies our previous investigation of statistical properties of $\tilde{\theta}_n$, as this is the limit converged by $\hat{\theta}_t$ through the SGD algorithm.*

5 Simulation Studies

5.1 Impact of Batch Size on the Local Convexity

We conduct simulation studies to evaluate how the local convexity of $\mathbb{E}[\nabla_{\theta}^2 L_{Cox}^{(s)}(\theta)]|_{\theta=\theta_0}$ changes with s in Cox-regression with $\theta \in \mathbb{R}^1$. We set $\theta_0 = 1$ and generated X from a uniform distribution $[0, 10]$. For each s , we estimate $\hat{\mathbb{E}}[\nabla_{\theta} L_{Cox}^{(s)}(\theta)]$ on a neighborhood of θ_0 from the average of 20,000 realizations of $\nabla_{\theta} L_{Cox}^{(s)}(\theta)$. Each realization consists of s i.i.d. time-to-event data (X_i, T_i, Δ_i) where T_i^* is from a Cox model with $f_0(X_i) = \theta_0 X_i$ and C_i^* is from an independent exponential distribution with censoring rate 45%.

Figure (1b) presents $\mathbb{E}[\nabla_{\theta} L_{Cox}^{(s)}(\theta)]$ in a neighborhood of $\theta_0 = 1$ (i.e., $\theta \in [0.90, 1.10]$) with different batch sizes s . As shown in Figure (1b), $\theta_0 = 1$ is always the root of $\mathbb{E}[\nabla_{\theta} L_{Cox}^{(s)}(\theta)]$ regardless the choice of s . Moreover, it verifies $\mathbb{E}[\nabla_{\theta}^2 L_{Cox}^{(2s)}(\theta)]|_{\theta=\theta_0} \geq \mathbb{E}[\nabla_{\theta}^2 L_{Cox}^{(s)}(\theta)]|_{\theta=\theta_0}$, given the increase in the slope of $\mathbb{E}[\nabla_{\theta} L_{Cox}^{(s)}(\theta)]$ at $\theta_0 = 1$ when the batch size doubles. The increment becomes negligible for large s , as discussed in Remark 10.

5.2 Impact of Batch Size in Cox Regression

We carried out simulations with 200 runs to empirically assess the impact of batch size in Cox regression. The true event time T_i^* is generated from $\lambda(t|X_i) = \lambda_0(t) \exp(X_i^T \theta_0)$ where $\lambda_0(t) = 1$, $\theta_0 = \mathbf{1}_{10 \times 1}$, and $X_{ip} \stackrel{i.i.d.}{\sim} \text{Uniform}(0,1)$ for $p \in \{1, 2, \dots, 10\}$. The true censoring time C_i^* is generated from an independent exponential distribution with a censoring rate 30%. We performed projected SGD (4.8) to estimate θ_0 based on $n = 2,048$ samples. The SGD batch size is 2^k where $k = 2, \dots, 9$. The total number of epochs (train the model with all the training data for one cycle) is 200 and the learning rate is set as $\gamma_E = \frac{2^{k-5}}{E+1}$ at epoch E , which is proportional to the batch size and decreases after each epoch. Besides SGD-SB and SGD-FB, we fit a stratified Cox model (CoxPH-strata) by treating the fixed

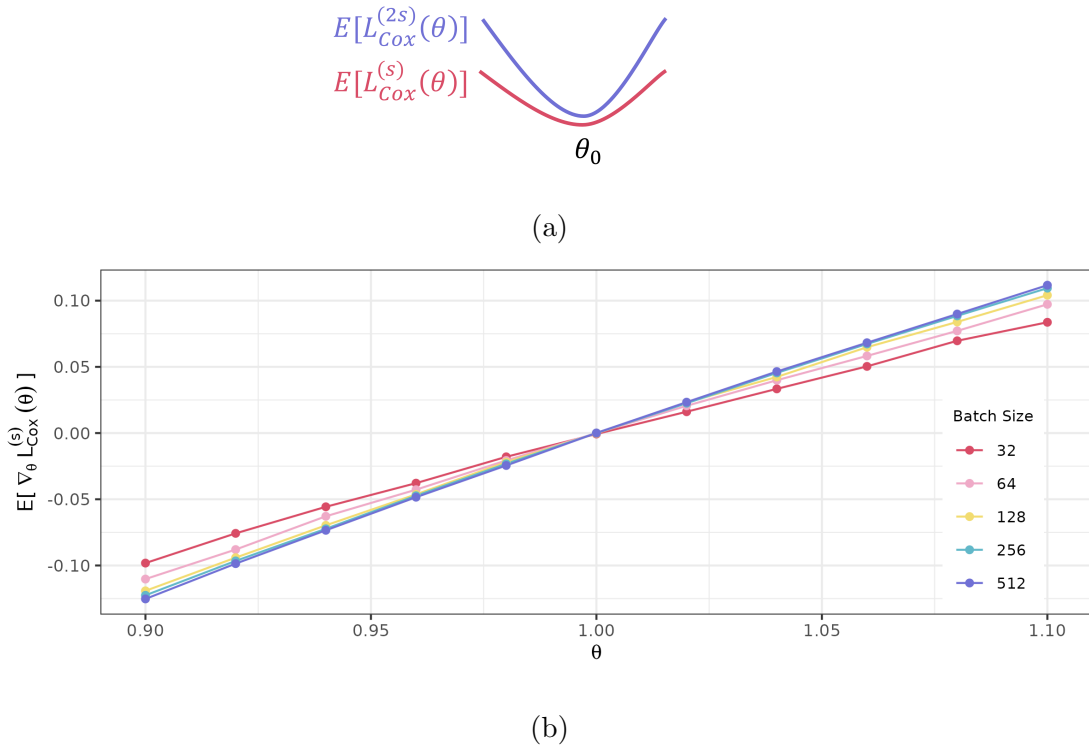


Figure 1: **(a)** An illustrative picture showing the properties of $\mathbb{E}[L_{Cox}^{(s)}(\theta)]$ in Cox-regression: $\mathbb{E}[L_{Cox}^{(s)}(\theta)]$ reaches the minimum at θ_0 regardless the choice of s while its local convexity at θ_0 increases when s doubles. **(b)** Estimated $\mathbb{E}[\nabla_{\theta} L_{Cox}^{(s)}(\theta)]$ at a neighborhood of $\theta_0 = 1$ with different batch sizes s . Each estimation is based on 20,000 realizations of the mini-batch data consisting of s i.i.d. samples generated from a Cox model with $f_0(X) = \theta_0 X$.

batches from SGD-FB as strata. Note that CoxPH-strata directly solves Eq. (4.3) using the GD algorithm. The convergence of the SGD algorithm can be evaluated by comparing the estimators from SGD-FB and CoxPH-strata. The MPLE (CoxPH) was also fitted.

The simulation results are presented in Figure 2. The convergence of SGD is validated by the negligible difference between the mb-MPLE $\hat{\theta}_t^{FB(s)}$ and the estimator from CoxPH-strata $\hat{\theta}^{strata}$ where $\log(\|\hat{\theta}^{FB(s)} - \hat{\theta}^{strata}\|_2^2) < -7.5$ for all s throughout the simulations. Since the bias is small, the level of $\|\hat{\theta} - \theta_0\|_2^2$ primarily reflects the variance of the estimator (see Supplementary Material for the bias, empirical variance, and asymptotic variance of

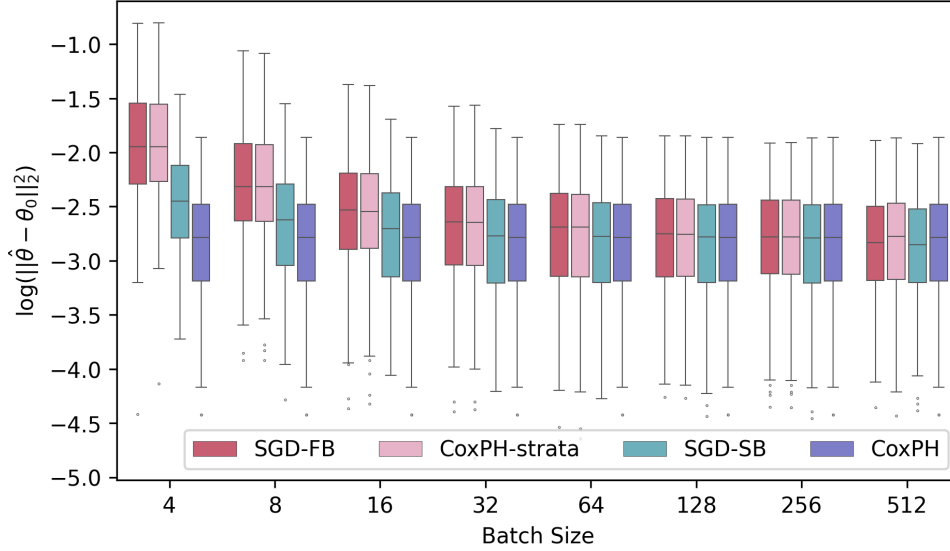


Figure 2: Boxplots of $\log(\|\hat{\theta} - \theta_0\|_2^2)$ over 200 runs with sample size $n = 2,048$ where $\hat{\theta}$ is solved by four different methods. SGD with two different batch sampling strategies is considered, either with a fixed batch sampling strategy (FB) or with a stochastic batch sampling strategy (SB). CoxPH-strata is a stratified Cox model treating the fixed batches from SGD-FB as strata and serves as the global minimizer for SGD-FB.

the estimators). Figure 2 shows that SGD-SB is more efficient than SGD-FB, especially when the batch size is small. There is an efficiency loss for both SGD-SB and SGD-FB compared to CoxPH. The efficiency loss becomes negligible when the batch size is large.

5.3 Linear Scaling Rule for Cox Neural Network

We further evaluated whether keeping the ratio of the learning rate to the batch size constant makes the SGD training process unchanged in Cox-NN. The data generating mechanism is the same as in Section 5.2 except that true event time T_i^* is generated from a Cox model with

$$f_0(X) = X_1^2 X_2^3 + \log(X_3 + 1) + \sqrt{X_4 X_5 + 1} + \exp(X_5/2) - 8.6, \quad X_p \sim U(0, 1), \quad p = 1, \dots, 5$$

where -8.6 is used to center $\mathbb{E}[f_0(X)]$ towards zero. A Cox-NN is fitted under different SGD learning rates and batch sizes. The full negative log-partial likelihood $L_{Cox}^{(N_{test})}$ was calculated on the same test data to reflect the training history. Identical to the spirit of [Goyal et al. \(2017\)](#), our goal is to match the test errors across batch sizes by only adjusting the learning rate. [Figure 3](#) shows that the linear scaling rule still holds in Cox-NN, especially when batch size is large (the three curves of batch size $s = 128, 256, 512$ are overlapped with each other). The differences between the curves (e.g., batch sizes 32 and 64) are due to the convexity change of the loss function when performing SGD with different batch sizes.

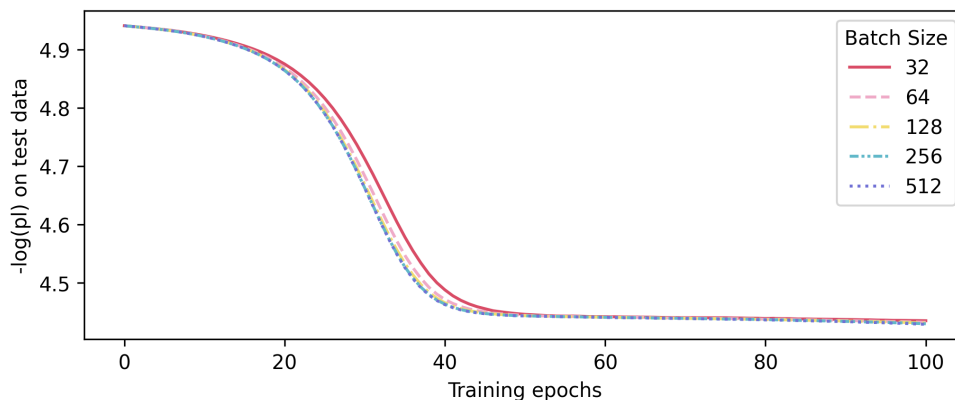


Figure 3: The negative log-partial likelihood $L_{Cox}^{(N_{test})}(\theta)$ evaluated on a test data ($N_{test} = 2,048$) over the training epochs. The learning rate γ is $0.1/16$ when the batch size is 32. γ is doubled when doubling the batch size. All the other hyperparameters are kept the same.

6 Real-world Data Analysis

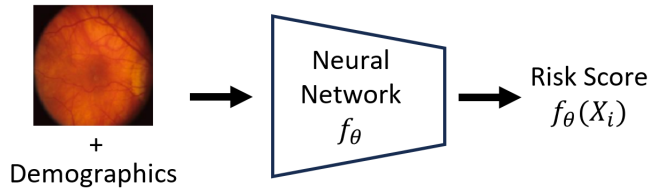
We applied the Cox-NN on the Age-Related Eye Disease Study (AREDS) data ([The Age-Related Eye Disease Study Research Group 1999](#)) and built a prediction model for a progressive eye disease, Age-related Macular Degeneration (AMD). The analysis data set includes 7,865 eyes of 4,335 subjects, with the outcome of interest being time from enrollment

(i.e., baseline) to progression to late AMD. The main predictor is the colored fundus image taken at the baseline. Other predictors include demographic variables (age at enrollment, educational level, and smoking status). There have been several existing works using fundus images to predict AMD progression. For example, Peng et al. (2020) implemented a two-step approach, where the first step is to fit a convolutional neural network on images with a binary outcome (progress vs not progress) to obtain a lower-dimensional predictor, and then the second step is to perform a Cox regression with this lower-dimensional image-based predictor from the first stage (together with other predictors) to predict time-to-progression. Our goal is to build a one-step prediction model by implementing Cox-NN directly on fundus images. The size of the raw fundus image is $3 \times 2300 \times 3400$. We cropped out the middle part of the fundus image and resized it to $3 \times 224 \times 224$. In this application, the Cox-NN employed the ResNet50 structure (He et al. 2016) to take the fundus image as input (shown in the first panel in Figure 4), which was optimized through SGD on a training set (7,087 samples) using a Nvidia L40s GPU with 48 GB memory and then evaluated the concordance index (C-index) by Harrell et al. (1982) in a separate test set (778 samples) to measure the predictive performance.

We first investigate the performance of SGD when optimizing a given Cox-NN (details in the Supplementary Material) under different batch sizes with a fixed learning rate ($\gamma = 0.002$). The second panel of Figure 4 presents the memory required to perform SGD with different choices of batch size. The memory required for SGD increases approximately linearly as the batch size grows, and is already 26.9 GB for a batch size of 256. The GD is equivalent to setting the batch size to 7,087 and is therefore not feasible in this application. Moreover, SGD with a smaller batch size leads to a shorter time to run an epoch and a faster learning process (as presented in the second and third panels of Figure 4).

Next, we verified the linear scaling rule by adjusting both the batch size and the learning

Cox Neural Network: $\lambda(t|X) = \lambda_0(t) \exp\{f_\theta(X)\}$



Optimize Cox model through SGD with batch size s : $\hat{\theta}_{t+1} = \hat{\theta}_t - \gamma_t \nabla_{\theta} L_{Cox}^{(s)}(f_{\hat{\theta}_t})$

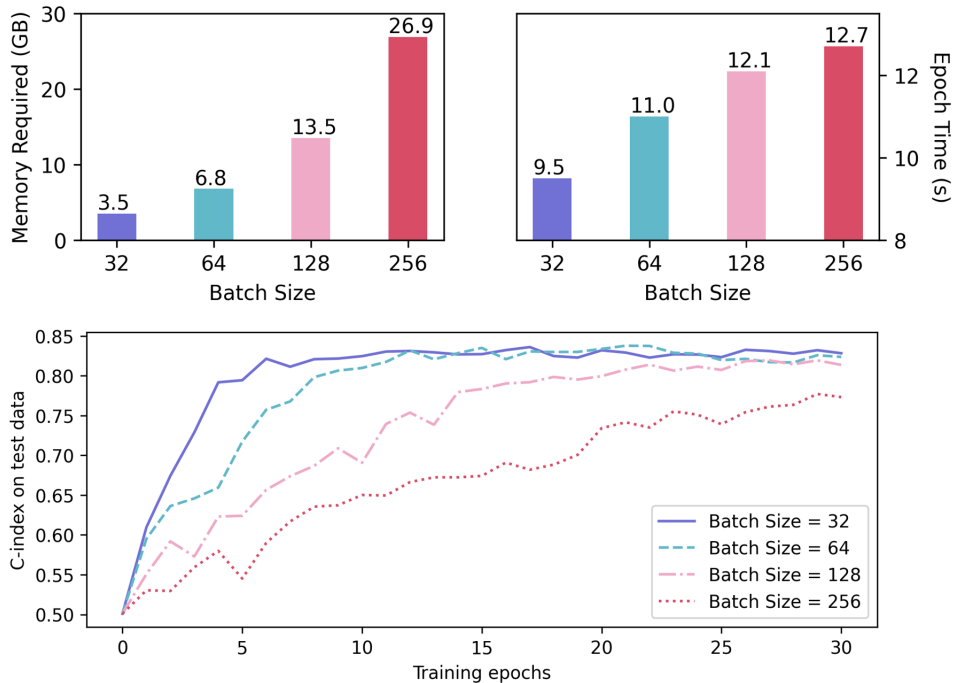


Figure 4: First panel: the structure of the Cox-NN model optimized by SGD to predict the time-to-AMD progression based on the fundus image and demographics; second panel: the required memory and running time of SGD over different batch sizes; third panel: the C-index (on the test data) over training epochs under the choice of different batch sizes.

rate of the SGD algorithm. From the trajectories of the C-index over the training epochs in Figure 5, the SGD training history would be similar when γ/s is the same. Moreover, reducing the batch size by half is equivalent to doubling the learning rate, which leads to faster convergence. For example, decreasing the batch size from 64 to 32 with a learning rate of 0.002 (dash-dotted line to dashed) or increasing the learning rate from 0.002 to 0.004 with a batch size of 64 (dash-dotted line to solid line) generates similar training

trajectories. This justifies our discussion in Section 3.2 that the ratio of learning rate to batch size γ/s determines the dynamics of SGD in Cox-NN training.

Lastly, we built a prediction model by fine-tuning the hyperparameters, such as the Cox-NN structures and SGD parameters, through a grid search. Guided by the linear scaling rule, we fixed the batch size to 32 and only tuned the learning rate. Detailed configurations of the hyperparameters are displayed in the Supplementary Material. To tune the hyperparameters, we held out a validation set (20%) from the 7,087 training data and evaluated the C-index on the validation set after training with different configurations. We chose the hyperparameters that maximized the C-index on the validation set for our final model, which achieved a C-index of 0.85 on the test data.

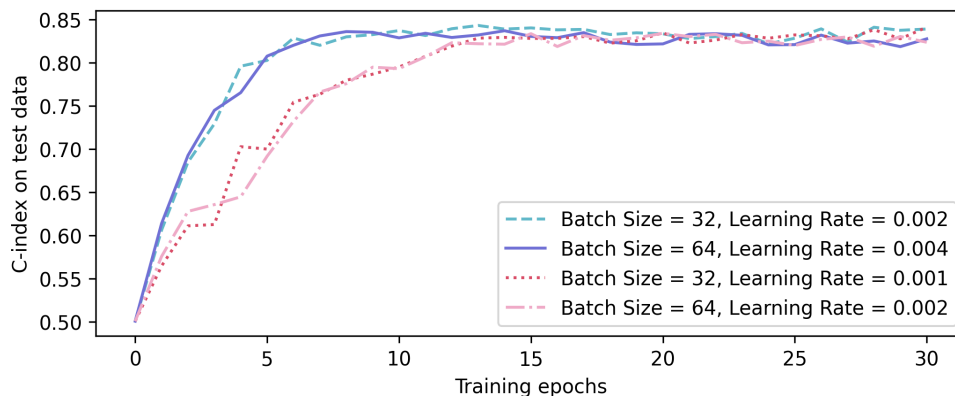


Figure 5: The C-index on test data of Cox-NN over training epochs in the AREDS application. The Cox-NN is optimized by SGD with different choices of batch size and learning rate. All the other hyperparameters are fixed.

7 Discussion

This paper studies the statistical properties of the mb-MPLE for deep Cox models, establishing its consistency and optimal convergence rate. We show that the SGD seeks to

optimize a function that depends on batch size, which differs from the all-sample partial likelihood. The paper investigates the properties of this batch-size-dependent function and presents the impact of SGD batch size in Cox-NN and regression. While we analyzed the optimization error of SGD in Cox regression, extending this analysis to Cox-NN is beyond the scope of the current work and remains an important direction for future research.

The partial likelihood in the Cox model essentially models the rank of event times through a Plackett-Luce (PL) model (Plackett 1975, Luce 1959) with censored outcome data. PL model with neural networks has been widely used in various tasks, such as learning-to-rank (LTR) (Cao et al. 2007) and contrastive learning (Chen et al. 2020). These applications are equivalent to applying Cox-NN to time-to-event data without right-censoring. Thus, our results and discussions can be extended to these tasks as a potential direction for future research.

References

- Amari, S. (1993), ‘Backpropagation and stochastic gradient descent method’, *Neurocomputing* **5**(4-5), 185–196.
- Andersen, P. K. & Gill, R. D. (1982), ‘Cox’s Regression Model for Counting Processes: A Large Sample Study’, *The Annals of Statistics* **10**(4), 1100–1120.
- Bauer, B. & Kohler, M. (2019), ‘On deep learning as a remedy for the curse of dimensionality in nonparametric regression’, *The Annals of Statistics* **47**(4), 2261–2285.
- Bottou, L. (2012), Stochastic Gradient Descent Tricks, *in* ‘Neural Networks: Tricks of the Trade: Second Edition’, Springer, pp. 421–436.

- Cao, Z. et al. (2007), Learning to Rank: From Pairwise Approach to Listwise Approach ,
in ‘Proceedings of the 24th international conference on Machine learning’, pp. 129–136.
- Chen, T. et al. (2020), A Simple Framework for Contrastive Learning of Visual Representations, *in* ‘International conference on machine learning’, PMLR, pp. 1597–1607.
- Ching, T. et al. (2018), ‘Cox-nnet: An artificial neural network method for prognosis prediction of high-throughput omics data’, *PLoS computational biology* **14**(4), e1006076.
- Choromanska, A., Henaff, M., Mathieu, M. et al. (2015), The loss surfaces of multilayer networks, *in* ‘Artificial intelligence and statistics’, PMLR, pp. 192–204.
- Cox, D. R. (1972), ‘Regression Models and Life-Tables’, *Journal of the Royal Statistical Society: Series B (Methodological)* **34**(2), 187–202.
- Cox, D. R. (1975), ‘Partial likelihood’, *Biometrika* **62**(2), 269–276.
- Faraggi, D. & Simon, R. (1995), ‘A neural network model for survival data’, *Stat Med.* **14**(1), 73–82.
- Goldstein, L. & Langholz, B. (1992), ‘Asymptotic Theory for Nested Case-Control Sampling in the Cox Regression Model’, *The Annals of Statistics* **20**(4), 1903–1928.
- Goyal, P. et al. (2017), ‘Accurate, Large Minibatch SGD: Training ImageNet in 1 Hour’, *arXiv preprint arXiv:1706.02677* .
- Harrell, F. E., Califf, R. M., Pryor, D. B., Lee, K. L. & Rosati, R. A. (1982), ‘Evaluating the Yield of Medical Tests’, *JAMA* **247**(18), 2543–2546.
- He, K., Zhang, X. et al. (2016), Deep Residual Learning for Image Recognition, *in* ‘Proceedings of the IEEE conference on computer vision and pattern recognition’, pp. 770–778.

- Hoeffding, W. (1992), ‘A Class of Statistics with Asymptotically Normal Distribution’, *Breakthroughs in statistics: Foundations and basic theory* pp. 308–334.
- Huang, J. (1999), ‘Efficient estimation of the partly linear additive cox model’, *The Annals of Statistics* **27**(5), 1536–1563.
- Jastrzebski, S., Kenton, Z., Arpit, D., Ballas, N., Fischer, A., Bengio, Y. & Storkey, A. (2017), ‘Three Factors Influencing Minima in SGD’, *arXiv preprint arXiv:1711.04623*.
- Katzman, J. L. et al. (2018), ‘DeepSurv: personalized treatment recommender system using a Cox proportional hazards deep neural network’, *BMC medical research methodology* **18**(1), 1–12.
- Kleinberg, B., Li, Y. & Yuan, Y. (2018), An Alternative View: When Does SGD Escape Local Minima?, *in* ‘International conference on machine learning’, PMLR, pp. 2698–2707.
- Kvamme, H., Borgan, Ø. & Scheel, I. (2019), ‘Time-to-Event Prediction with Neural Networks and Cox Regression’, *Journal of Machine Learning Research* **20**, 1–30.
- Li, H., Xu, Z., Taylor, G., Studer, C. & Goldstein, T. (2018), ‘Visualizing the Loss Landscape of Neural Nets’, *Advances in neural information processing systems* **31**.
- Luce, R. D. (1959), *Individual choice behavior*, Vol. 4, Wiley New York.
- Moulines, E. & Bach, F. (2011), ‘Non-asymptotic analysis of stochastic approximation algorithms for machine learning’, *Advances in neural information processing systems* **24**.
- Nair, V. & Hinton, G. E. (2010), Rectified Linear Units Improve Restricted Boltzmann Machines, *in* ‘Proceedings of the 27th international conference on machine learning (ICML-10)’, pp. 807–814.

- Peng, Y., Keenan, T. D. et al. (2020), ‘Predicting risk of late age-related macular degeneration using deep learning’, *npj Digit. Med.* **3**(1), 111.
- Plackett, R. L. (1975), ‘The Analysis of Permutations’, *Journal of the Royal Statistical Society Series C: Applied Statistics* **24**(2), 193–202.
- Polyak, B. T. & Juditsky, A. B. (1992), ‘Acceleration of Stochastic Approximation by Averaging’, *SIAM journal on control and optimization* **30**(4), 838–855.
- Qi, H., Wang, F. & Wang, H. (2023), ‘Statistical Analysis of Fixed Mini-Batch Gradient Descent Estimator’, *Journal of Computational and Graphical Statistics* **32**(4), 1348–1360.
- Ruppert, D. (1988), Efficient estimations from a slowly convergent Robbins-Monro process, Technical report, Cornell University Operations Research and Industrial Engineering.
- Schmidt-Hieber, J. (2020), ‘Nonparametric regression using deep neural networks with ReLU activation function’, *The Annals of Statistics* **48**(4), 1875–1897.
- Srinivas, S. et al. (2017), Training Sparse Neural Networks, in ‘Proceedings of the IEEE conference on computer vision and pattern recognition workshops’, pp. 138–145.
- Srivastava, N., Hinton, G. et al. (2014), ‘Dropout: A Simple Way to Prevent Neural Networks from Overfitting’, *Journal of Machine Learning Research* **15**(1), 1929–1958.
- Sun, T., Wei, Y., Chen, W. & Ding, Y. (2020), ‘Genome-wide association study-based deep learning for survival prediction’, *Stat Med.* **39**(30), 4605–4620.
- Tarkhan, A. & Simon, N. (2024), ‘An online framework for survival analysis: reframing Cox proportional hazards model for large data sets and neural networks’, *Biostatistics* **25**(1), 134–153.

- The Age-Related Eye Disease Study Research Group (1999), ‘The Age-Related Eye Disease Study (AREDS): Design Implications AREDS Report No. 1’, *Controlled clinical trials* **20**(6), 573–600.
- Therneau, T. et al. (2015), ‘A package for survival analysis in R’, *R package version* **2**(7), 2014.
- Toulis, P. & Airolidi, E. M. (2017), ‘Asymptotic and finite-sample properties of estimators based on stochastic gradients’, *The Annals of Statistics* **45**(4), 1694–1727.
- Tsiatis, A. A. (2006), *Semiparametric theory and missing data*, Vol. 4, Springer.
- Xie, Z. et al. (2020), ‘A Diffusion Theory For Deep Learning Dynamics: Stochastic Gradient Descent Exponentially Favors Flat Minima’, *arXiv preprint arXiv:2002.03495* .
- Zhong, Q., Mueller, J. & Wang, J.-L. (2022), ‘Deep learning for the partially linear Cox model’, *The Annals of Statistics* **50**(3), 1348–1375.